

RESEARCH

Open Access



# Tppp3 is a novel molecule for retinal ganglion cell identification and optic nerve regeneration

Mishal Rao<sup>1</sup> , Ziming Luo<sup>2</sup>, Chia-Chun Liu<sup>1</sup>, Chi-Yu Chen<sup>1</sup>, Shining Wang<sup>1</sup>, Michael Nahmou<sup>2</sup>, Bogdan Tanasa<sup>2</sup>, Aman Virmani<sup>1</sup>, Leah Byrne<sup>1,3,4</sup>, Jeffrey L. Goldberg<sup>2</sup>, José-Alain Sahel<sup>1</sup> and Kun-Che Chang<sup>1,2,3,4,5\*</sup> 

## Abstract

Mammalian central nervous system (CNS) axons cannot spontaneously regenerate after injury, creating an unmet need to identify molecular regulators to promote axon regeneration and reduce the lasting impact of CNS injuries. While tubulin polymerization promoting protein family member 3 (Tppp3) is known to promote axon outgrowth in amphibians, its role in mammalian axon regeneration remains unknown. Here we investigated Tppp3 in retinal ganglion cells (RGCs) neuroprotection and axonal regeneration using an optic nerve crush (ONC) model in the rodent. Single-cell RNA sequencing identified the expression of Tppp3 in RGCs of mice, macaques, and humans. Tppp3 overexpression enhanced neurite outgrowth in mouse primary RGCs in vitro, promoted axon regeneration, and improved RGC survival after ONC. Bulk RNA sequencing indicated that Tppp3 overexpression upregulates axon regeneration genes such as Bmp4 and neuroinflammatory pathways. Our findings advance regenerative medicine by developing a new therapeutic strategy for RGC neuroprotection and axon regeneration.

**Keywords** Tppp3, Retinal ganglion cells, Axon regeneration, Neurite outgrowth, BMP4, Inflammation

## Introduction

Injury to the central nervous system (CNS) axons is a hallmark of many neurodegenerative diseases such as glaucoma and traumatic brain injury [19]. In mammals, CNS axons cannot spontaneously regenerate over long

distances following injury, leading to functional loss and axonal degeneration [15]. Conversely, peripheral nervous system neurons can intrinsically re-activate pro-regenerative signaling mechanisms to regenerate axons spontaneously [45]. The intrinsic properties of CNS neurons and the inhibitory environment of the CNS contribute to impeding axon regeneration [17, 40]. Therefore, there is an unmet need to identify molecules that stimulate axon regeneration over long distances in the CNS to recover functionality after injury.

The visual system is an advantageous model for studying axon regeneration due to its accessibility and functional importance [5]. It includes retinal ganglion cells (RGCs), which are CNS neurons that relay visual information from the eyes to the brain via their axons, which form the optic nerve. Optic neuropathies, such as Leber's Hereditary Optic Neuropathy, are characterized by damage to the optic nerve and pose a significant challenge to

\*Correspondence:

Kun-Che Chang  
kcchang@pitt.edu

<sup>1</sup> Department of Ophthalmology, UPMC Vision Institute, University of Pittsburgh School of Medicine, 1622 Locust Street, Pittsburgh, PA 15219, USA

<sup>2</sup> Spencer Center for Vision Research, Byers Eye Institute, Stanford University, Stanford, CA 94305, USA

<sup>3</sup> Department of Neurobiology, Center of Neuroscience, University of Pittsburgh School of Medicine, Pittsburgh, PA 15213, USA

<sup>4</sup> Department of Bioengineering, University of Pittsburgh, Pittsburgh, PA 15213, USA

<sup>5</sup> Graduate Institute of Medicine, College of Medicine, Kaohsiung Medical University, Kaohsiung 80708, Taiwan



© The Author(s) 2024. **Open Access** This article is licensed under a Creative Commons Attribution-NonCommercial-NoDerivatives 4.0 International License, which permits any non-commercial use, sharing, distribution and reproduction in any medium or format, as long as you give appropriate credit to the original author(s) and the source, provide a link to the Creative Commons licence, and indicate if you modified the licensed material. You do not have permission under this licence to share adapted material derived from this article or parts of it. The images or other third party material in this article are included in the article's Creative Commons licence, unless indicated otherwise in a credit line to the material. If material is not included in the article's Creative Commons licence and your intended use is not permitted by statutory regulation or exceeds the permitted use, you will need to obtain permission directly from the copyright holder. To view a copy of this licence, visit <http://creativecommons.org/licenses/by-nc-nd/4.0/>.

visual health. Following optic nerve injury, RGCs cannot re-activate or reprogram developmental growth signaling pathways to promote axon regeneration [53]. Current treatments for RGC-related conditions are limited, emphasizing the urgent need for innovative therapeutic approaches to promote RGC survival and protect visual function [57]. In recent years, gene therapy has emerged as a promising avenue to address optic neuropathies. Thus, identifying genes involved in RGC survival and regeneration is key to developing targeted therapeutic strategies.

In this study, we investigated the role of tubulin polymerization promoting protein family member 3 (*Tppp3*) as a candidate gene to enhance RGC survival and axon regeneration. TPPP3, also known as p20 or cyclin-dependent kinase inhibitor 1d, acts as a microtubule-associated protein by binding to and contributing to tubulin polymerization and microtubule stabilization [21, 32, 34, 55]. TPPP3s are also critical for elongation of the myelin sheath [16, 54], an essential glial component of the optic nerve [61]. Moreover, *Tppp3* promotes axon regeneration in zebrafish [20]. Since stabilizing microtubules improves the transport of essential elements to the growth cone [8, 31] and TPPP3 appears to play a role in regulating microtubule dynamics and neuronal function [1, 20], TPPP3 could potentially have a positive role in mammalian axon regeneration. Here, we tested the hypothesis that *Tppp3* overexpression could promote axon regeneration and RGC survival in a mouse optic nerve crush (ONC) model. TPPP3 functions as a regulator to stimulate the intrinsic regenerative ability of RGCs, which could have a translational impact on regenerative medicine and lead to the development of a new therapeutic to promote optic nerve regeneration after injury.

## Materials and methods

### Animals

All animal experiments adhered to guidelines set forth by the Association for Research in Vision and Ophthalmology as well as Animal Research: Reporting of In Vivo Experiments. Animal experiments were approved by the Institutional Animal Care and Use Committees of the University of Pittsburgh and Stanford University. We used both male and female C57BL/6 mice for this research.

### Single-cell RNA sequencing

E14.5 mouse retinas were dissociated using papain (#LK003150, Worthington) and re-suspended in retinal progenitor cell (RPC) media. RPC media comprised of glucose (0.6%, Sigma), GS21 (1:100, GlobalStem), Sato supplement (1:100), insulin (5 µg/mL, Sigma), epidermal growth factor (20 ng/mL, Peprotech), fibroblast growth

factor (20 ng/mL, Peprotech), penicillin/streptomycin (1%, Thermo Fisher Scientific) suspended in DMEM/F12 medium. The dissociated cells were plated on poly-D-lysine-(PDL)/Laminin-coated dishes. Cells were treated with 50 ng/mL mouse growth differentiation factor 11 (GDF11), or PBS for 5 days. GDF 11 was purchased from R & D systems (#1958-GD-010/CF). Treated cells were then dissociated by Accutase (Innovative Cell Technologies) for 15–20 min on day 6. Cell pellets were filtered through a 40µm cell strainer (Falcon, #352,340) and resuspended in PBS with 0.04% BSA. We targeted 10,000 cells for 10X capturing. GEM generation, reverse transcription, cDNA amplification, and library constructions were performed following the manufacturer's instructions (Chromium Single Cell 3'v1/v2/v3 platform, 10X Genomics, Pleasanton, CA). Samples were sequenced on an Illumina NextSeq 500.

We applied FASTQ with the default parameters, filtering the adaptor sequence and achieving clean data by removing the low-quality reads. Then, we obtained the feature-barcode matrices by aligning reads to the mm10 genome using CellRanger v3.0.0. Seurat analysis was performed in R using Seurat (v3.2.0), ggplot2, and dplyr. We first log normalized the data and identified variable features by scaling gene content by cells. Different treatment datasets (i.e. GDF11, and control) were integrated by identifying 'anchors' across datasets; the data was scaled subsequently. Cell clusterings were visualized by tSNE dimensional reduction in Fig. 1. In Fig. 1D, the RGC population was identified by marker gene *Pou4f1*. Then, the *Tppp3* expression level was visualized specifically in the RGC subset (GSE252861).

In this study, we also re-analyzed previously published scRNA sequencing data sets. scRNA sequencing data were accessed on Gene Expression Omnibus (GEO) under accession numbers GSE199840 (human retina data), GSE161645 (macaque retina data), and GSE137400 (mouse RGC data and ONC). Furthermore, Broad Institute's Single Cell Portal website was utilized for data visualization of the mouse RGC dataset after ONC- GSE137400.

### Adeno-associated virus (AAV) preparation

Adeno-associated virus type 2 vectors driving *Tppp3* overexpression- CMV > m*Tppp3*(overexpression): P2A:EGFP (AAV2-*Tppp3*-OE), *Tppp3* knockdown CMV > m*Tppp3*(shRNA):P2A:EGFP (AAV2-sh*Tppp3*) or cytomegalovirus (CMV) control (AAV2-control and AAV2-shCtrl) were purchased from VectorBuilder. Both the AAV2-control virus and the AAV2-shCtrl virus vector sequences include GFP and are driven by the CMV promoter. AAV2-shCtrl contains a scramble sequence. The plasmids were sent to AAVnerGene for AAV packaging

and purification (Rockville, MD, USA). The AAV2 vectors were produced with 293 T cells and purified using CsCl gradient ultracentrifugation. Vector genome concentration was titered by quantitative real-time PCR with iTR primers and digested plasmid as standard (AAV2-Tppp3-OE:  $6.92 \times 10^{11}$  vg/mL, AAV2-control:  $8.95 \times 10^{11}$  vg/mL, AAV2-shTppp3:  $7.29 \times 10^{11}$  vg/mL, AAV2-shCtrl:  $5.05 \times 10^{11}$  vg/mL).

### Western blot

Protein samples were collected from primary RGCs purified from P2 mouse pups by immunostaining based on the expression of CD90.1 as previously described [4]. The remaining non-RGC cells collected while immunopanning were used as the RGC-depleted population. Samples were collected using Laemmli sample buffer (Sigma-Aldrich, St. Louis, MO, USA). Protein lysates were heated at 100 °C for 10 min, loaded onto precast SDS-PAGE gels (Bio-Rad, Hercules, CA, USA), and run to achieve complete protein separation. A semi-dry blotter from Bio-Rad was used to transfer proteins onto polyvinylidene difluoride membranes. Membranes were blocked for 1 h at room temperature using LI-COR Intercept Blocking Buffer (LI-COR Biosciences, Lincoln, NE, USA).

Membranes were incubated overnight at 4 °C with primary antibodies in LI-COR Intercept Antibody Buffer for immunodetection. Primary antibodies used included those to BRN3A (1:500, MAB1585, Millipore Sigma, Burlington, MA), THY1 (1:500, #5568S, Cell Signaling), RBPMS (1:500, #1832, PhosphoSolutions, Aurora, CO, USA), TPPP3 (1:500, PA5-24,925, Invitrogen, Waltham, MA, USA), and GAPDH (1:500, #2118S, Cell Signaling). Following primary antibody incubation, membranes were incubated with species-specific secondary antibodies linked to near-infrared dyes (#926–68,072, IRDye 680RD donkey anti-mouse; #926–3211, IRDye 800CW goat anti-rabbit; LI-COR Biosciences) at a dilution of 1:10,000 for 4 h at room temperature. Membranes were washed and imaged on a LI-COR Odyssey IR using a linear range detection system.

HeLa cells, obtained from ATCC, were cultured in Eagle's Minimum Essential Medium supplemented with 10% fetal bovine serum, maintained at 37 °C with 5% CO<sub>2</sub>. The cells were first transduced with either AAV2-Tppp3-OE or AAV2-control for two days. Following this initial treatment, to test the shRNA transduction efficiency, AAV2-Tppp3-OE-transduced cells were treated with either AAV2-shTppp3 or AAV2-shCtrl, while AAV2-control-transduced cells received AAV2-shCtrl. After treatment, the cells were harvested as previously described and probed for Tppp3 and GAPDH expression.

### Immunostaining

Eye globes were fixed with 4% paraformaldehyde (PFA) at 4 °C overnight, then incubated in 15% sucrose at 4 °C overnight and 30% sucrose at 4 °C overnight before mounting in Optimal Cutting Temperature mounting medium (Thermo Fisher Scientific, Waltham, MA, USA). 10 μm-thick cryosections were cut from the embedded eye globe. Sections were incubated in blocking buffer containing 5% normal goat serum (NGS) and 0.1% Triton X-100 in PBS for 1 h at room temperature. After three PBS washes, sections were incubated overnight at 4 °C with primary antibodies to mouse Brn3a (1:100, Millipore Sigma, Burlington, MA), mouse anti-β-III-tubulin antibody E7 (1:500, hybridoma from Developmental Studies Hybridoma Bank), and rabbit anti-Tppp3 (1:200, PA5-24,925, Invitrogen).

Following overnight incubation, sections were incubated with secondary antibodies for 4 h at room temperature. We used Alexa Fluor 488 goat anti-rabbit (1:500, #A11034, Life technologies), Alexa Fluor 647 anti-mouse (1:500, A-1235, Life Technologies) and 4',6-diamidino-2-phenylindole (DAPI) (1:500, #D9542, Sigma-Aldrich). Images were captured on an Olympus Life Science IX83 inverted microscope.

### RNAscope in situ hybridization (ISH)

In situ detection of Tppp3 mRNA on mouse tissue was performed by a manual method using the RNAscope kit (Advanced Cell Diagnostics) as previously described [11]. Briefly, 12 μm OCT-frozen tissue sections (E12, E14, E18,

(See figure on next page.)

**Fig. 1** Identification of Tppp3 by single-cell RNA sequencing. **A** Schematic representation of the Experimental design for single-cell RNA sequencing (scRNA-seq) conducted on E14.5 retina samples treated with GDF11 or PBS. **B** t-distributed stochastic neighbor embedding (t-SNE) visualization of retinal progenitor cells, with cells color-coded based on their cluster assignments and treatment conditions. Cluster 3 represents the RGC cluster. **C** GDF11, RGC fate suppressor protein, leads to a reduction in the expression levels of *Pou4f1* and *Tppp3*, specifically within the RGC cluster (cluster 3). This highlights the potential role of Tppp3 in RGC differentiation. **D** *Pou4f1* expression is specifically localized within cluster 3, identified as the RGC-specific cluster. **E** *Tppp3* is also highly expressed within cluster 3. **F** Violin plot displaying the expression level of *Tppp3* from a reanalysis of scRNA data obtained from purified RGCs. The X-axis represents the time points following optic nerve crush, while the numbers above the violin plots indicate the percentage of RGCs expressing Tppp3. 2 weeks after ONC, Tppp3 expression is reduced substantially. Tppp3 is highly expressed within the RGC clusters of **G** macaque and **H** humans

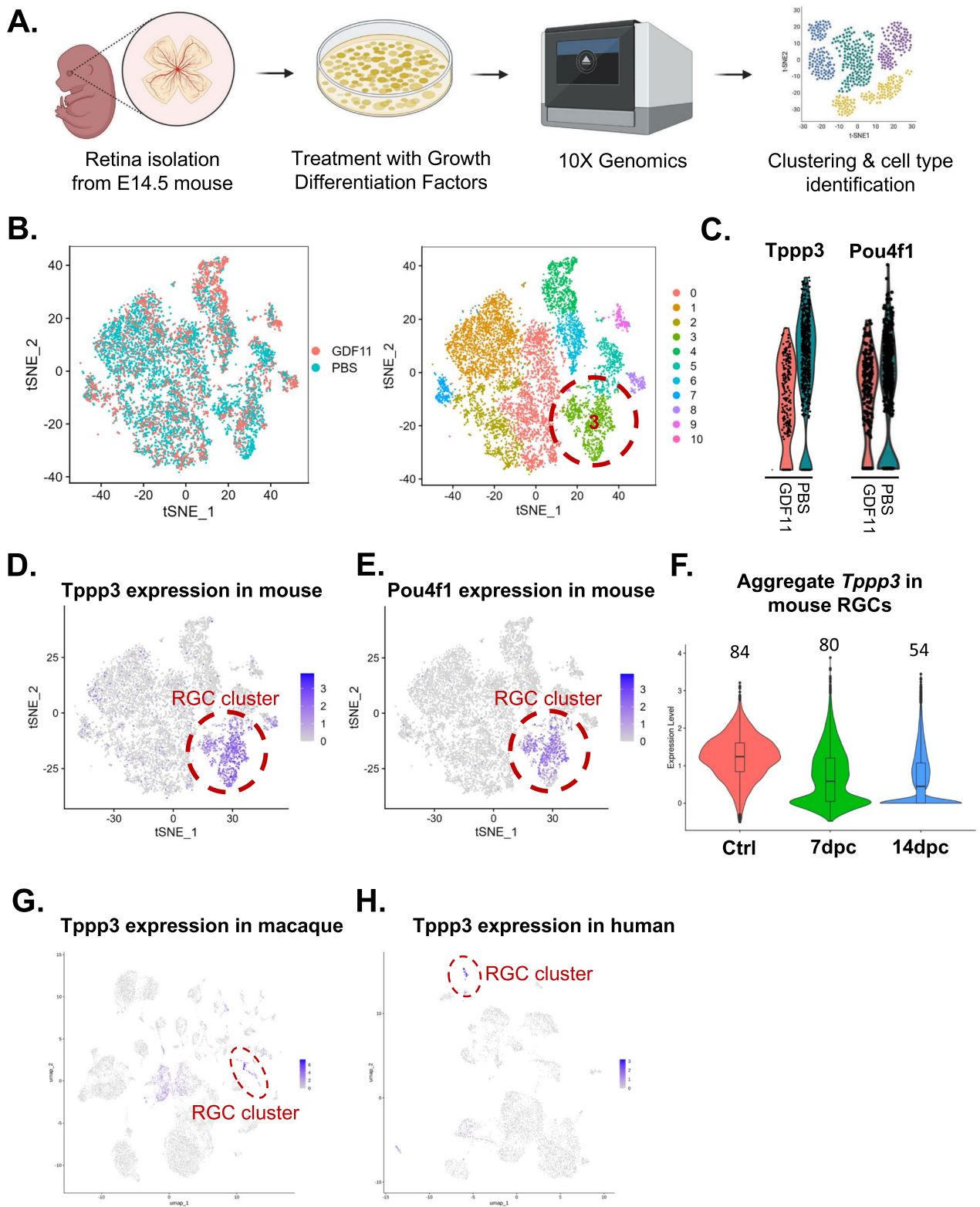


**Fig. 1** (See legend on previous page.)

and P0) were pretreated with hydrogen peroxide, antigen retrieval, and protease application before hybridization with a target probe to mouse *Tppp3*. Incubation processes were followed by the manufacturer's instructions. Colorimetric substrate (red) was added to sections and incubated for 10 min at room temperature for observation. Multiple tissues were tested and individual representative sections were shown.

#### RGC culture and neurite outgrowth

Primary mouse RGCs were purified from postnatal day 2 pups by immunopanning using immobilized antibodies against CD90.1 as previously described [4]. Primary RGCs were plated in a 24-well plate at a density of  $2.5 \times 10^3$  RGCs/well onto PDL/laminin-coated tissue culture plates. Full Sato medium which included forskolin (5 mM), BDNF (50 ng/mL), and CNTF (10 ng/mL) was used for neurite outgrowth assays. The purity of immunopanned RGCs was validated through immunostaining with Tuj1, Brn3a, and DAPI. As shown in Supplementary Fig. 5, the majority of cells were confirmed to be RGCs. For viral transduction, AAV2-*Tppp3*-OE or AAV2 control was added to the culture medium at a multiplicity of infection of  $\sim 10^5$  vg/cell 24 h. Similarly, AAV2-sh*Tppp3* or AAV2-shCtrl were added to the culture medium. The virus was removed after 24 h and RGCs were incubated for 2 days in fresh medium.

For immunostaining, RGCs were fixed in 4% PFA directly added to the culture medium (2% final PFA dilution) for 20 min. Neurites were blocked in 5% NGS and 0.1% Triton X-100 in PBS for 1 h at room temperature. Rabbit Tuj-1 (1:500; #5568S, Cell Signaling) was used to stain neurites overnight and was visualized with an Alexa Fluor 555-conjugated Goat Anti-rabbit IgG antibody (1:500, # A-21428, Life Technologies) for 4 h at room temperature. Neurite outgrowth was measured using an Olympus Life Science IX83 Inverted Microscope. Each image was taken at the same intensity and 10X magnification. For each treatment,  $\sim 30$  cells were averaged per condition for each experiment. The total length of neurites per cell was measured using ImageJ Simple Neurite Tracer. All imaging and quantification were conducted in a blinded manner to eliminate bias.

#### Optic nerve crush (ONC)

Adeno-associated virus type 2 vectors driving *Tppp3* overexpression (AAV2-*Tppp3*-OE) or cytomegalovirus control (AAV2-control) were intravitreally injected into the left eye two weeks before ONC. ONC was performed as previously described [9]. Ketamine/xylazine anesthesia was administered to 8–10-week-old mice. The left eye was subjected to ONC—the outer canthus was exposed, and the optic nerve was pinched for 7 s using Dumont

#5 self-closing forceps (Fine Science Tools, Foster City, CA, USA),  $\sim 1.5$  mm behind the globe. The right eye was left uninjured to serve as a control. At 12 days after ONC, 2  $\mu$ L of cholera toxin subunit B (CTB)-conjugated Alexa Fluor 555 (CTB-555) (2  $\mu$ g/ $\mu$ L, #C22843, Invitrogen) were intravitreally injected as an anterograde tracer. Animals were euthanized 14 days after ONC and perfused with 4% PFA before collecting optic nerves and retinas.

#### Quantitative real-time PCR (qPCR)

We isolated total RNA from retinal tissues collected from E12-P0, two days after ONC and two weeks using a Qiagen RNeasy Mini Kit per the manufacturer's protocol (Qiagen, Hilden, Germany). Reverse transcription of RNA (500 ng) was performed using the Bio-Rad iScript cDNA Synthesis Kit. qPCR was conducted using either Taqman master mix or Bio-Rad iTaq Universal SYBR-Green Supermix per the manufacturer's instructions. SYBR green primers for *Bmp4* and *Gapdh* were purchased from Integrated DNA Technologies (Coralville, IA, USA). All experiments were performed in triplicate to ensure accuracy and reproducibility.

#### RGC survival analysis

RGC survival was evaluated according to an established protocol [10]. First, retinas were dissected and fixed in 4% PFA for 1 h. To ensure complete permeabilization, retinas were treated with a solution containing 3% Triton X-100 (Sigma-Aldrich) and 1.5% Tween 20 (Sigma-Aldrich) for 1 h. Blocking was performed using 10% normal goat serum in PBS for 1 h. Retinas were incubated overnight at 4 °C with a rabbit polyclonal anti-RBPMS primary antibody (1:500, #1830, PhosphoSolutions). Following three washes with PBS (10 min each), retinal flatmount samples were incubated overnight with Alexa Fluor 647-goat anti-rabbit secondary antibody (1:500, #A21244, Life Technologies). After two additional washes (10 min each), samples were stained with DAPI (1:5000 in PBS) for 15 min. For preservation, samples were sealed under 1.5-mm coverslips using an anti-fade mounting medium (ProLong Gold, Life Technologies). Samples were imaged on a Zeiss fluorescence microscope (Oberkochen, Germany). Each retina was divided into four quadrants, and one random digital micrograph was captured from each peripheral area located 3 mm from the optic nerve head. RBPMS-positive (RBPMS+) cells were manually counted in a masked manner. Results are presented as cells per square millimeter.

#### Regenerative axon counting

For axon counting, optic nerves were collected two weeks after ONC, fixed in PFA for 1 h at room temperature, and washed in PBS. Optic nerves were immersed in 15%

sucrose at 4 °C overnight, followed by 30% sucrose at 4 °C overnight before mounting in Optimal Cutting Temperature mounting medium (Thermo Fisher). Cryosections 10- $\mu$ m thick were prepared for both the optic nerve and retina. Optic nerve sections were imaged and analyzed as described previously [9]. The number of CTB-positive axons (CTB+) within every 200  $\mu$ m, 600  $\mu$ m, 1000  $\mu$ m and 1600  $\mu$ m from the injury site were manually counted until the end of the longest regenerating axons. The total number of CTB+ axons per optic nerve was calculated using an established formula [23]. All imaging and quantification were conducted in a masked manner.

### RNA sequencing

RNA sequencing was performed to investigate gene expression profiles in the injured retina two days after ONC. Mouse retinas treated with either AAV2-Tppp3-OE (n=4) or AAV2-CMV (n=3) were dissected, and total RNA was extracted from the injured retinas. Total RNA was extracted from frozen retina samples using a Qiagen RNeasy Mini Kit per the manufacturer's instructions. Sample preparation was conducted in triplicate to ensure robustness and reproducibility.

Azenta Life Sciences (South Plainfield, NJ, USA) conducted sample, library preparation, and quality control analyses. Briefly, RNA samples were quantified using a Qubit 2.0 fluorometer (Life Technologies), and RNA integrity was checked using a TapeStation 4200 (Agilent Technologies, Palo Alto, CA, USA). ERCC RNA Spike-In Mix Kit (#4,456,740, Thermo Fisher Scientific) was added to normalized total RNA before library preparation following the manufacturer's protocol. RNA sequencing libraries were prepared using the NEBNext Ultra II RNA Library Prep Kit for Illumina per the manufacturer's instructions (New England Biolabs, Ipswich, MA, USA). Sequencing libraries were validated on an Agilent TapeStation and quantified using a Qubit 2.0 fluorometer (Thermo Fisher Scientific) as well as by quantitative PCR (KAPA Biosystems, Wilmington, MA, USA). Sequencing libraries were clustered on one flow cell lane. After clustering, the flow cell was loaded on an Illumina 4000 or equivalent instrument according to the manufacturer's instructions (Illumina, San Diego, CA, USA). Samples were sequenced using a 2 $\times$ 150 bp paired-end configuration. Raw sequence data (.bcl files) were converted into FASTQ files and de-multiplexed using Illumina bcl2fastq 2.17 software. One mismatch was allowed for index sequence identification.

The resulting FASTQ files were analyzed using CLC Genomics Workbench v22 from Qiagen Digital Insights. Raw sequencing reads were imported into the software for analysis, including identifying differentially expressed genes between AAV2-Tppp3-OE and AAV2-CMV

groups two days after ONC. The imported reads underwent quality checks, adaptor sequence trimming, and alignment to the GRCm39/mm39 version of the mouse reference genome using default settings. Quality checks were performed on mapped reads as well.

To determine the differential expression of genes between groups, a significance threshold of  $p \leq 0.05$  and fold-change >2 were used. Adjusted p-values were not used to compute differentially expressed genes in this analysis. Volcano plots were generated using CLC Genomics Workbench v22 to visualize results. Pathway enrichment analyses were conducted using the NIH Database for Annotation, Visualization, and Integrated Discovery 2021 with the Kyoto Encyclopedia of Genes and Genomes database. RNA sequencing data generated from this analysis have been deposited in Gene Expression Omnibus (GEO) under accession number GSE24244756.

### Statistical analysis

Statistical analysis was performed by calculating the mean  $\pm$  standard error of the mean (SEM) of at least three independent experiments. The number of mice used in each experiment is indicated in the figure legends. One-way ANOVA followed by post hoc t-tests with Tukey's correction and/or unpaired t-tests was used for data analysis, considering  $p < 0.05$  as significant. Graphs were created using Prism 9 software (GraphPad, La Jolla, CA, USA).

## Results

### Identification of Tppp3 as an RGC marker by single-cell RNA sequencing

To understand the gene expression dynamics governing the regulation of RGC fate differentiation, we conducted single-cell RNA sequencing (scRNA-seq) on mouse retinal progenitor cells (Fig. 1A) that were subjected to either PBS or growth and differentiation factor 11 (GDF11). GDF 11 is a known regulator of RGC differentiation and is recognized as a suppressor of RGC fate [11]. We collected retinas from E14.5 mice, a stage characterized by the peak of RGC differentiation [64], and treated them with GDF11 or PBS for 5 days to profile the retinal progenitor cells.

Our scRNA-seq analysis revealed the presence of 11 distinct clusters of retinal cells (Fig. 1B), with cluster 3 identified as the RGC cluster based on the expression of the RGC-specific gene *Pou4f1* (Fig. 1B and E). Additionally, other RGC marker genes like *Thy1*, *RBPMS*, and *Nefl* exhibited high expression within cluster 3 as well (data not shown). Notably, *Tppp3* was highly expressed in the RGC-specific cluster 3 (Fig. 1D). Further examination of gene expression levels indicated that GDF-11

treatment led to a reduction in the expression of both *Pou4f1* and *Tppp3*, specifically within the RGC clusters, identified as cluster 3 (Fig. 1C). RGC marker genes like *Sncg*, *Isl1*, and *Rbpms* were also downregulated after GDF11 treatment (data not shown). The localized expression of *Tppp3* within the RGC cluster and its modulation by GDF11 indicate its potential as a candidate gene for further investigation within RGCs.

Upon reanalyzing a previous scRNA-seq study [53] conducted on purified mouse RGCs, we observed a strikingly high expression of *Tppp3* within RGCs, with approximately 84% of the total RGC population expressing *Tppp3* (Fig. 1F). Moreover, reanalysis of scRNA-seq data from adult macaque and human retinas revealed that *Tppp3* is highly expressed within RGC clusters [35, 59] (Fig. 1G, H, and Supplementary Fig. 1). Given its widespread expression across RGCs of mice, macaque, and humans, it further emphasizes its potential role in RGC function.

As *Tppp3* expression was downregulated by the RGC fate suppressor protein GDF11 (Fig. 1C), and previous studies have linked *Tppp3* to RGCs and zebrafish axon regeneration [20], we next investigated the gene and protein profiles of *Tppp3* in vivo and studied its potential role in regulating optic nerve regeneration.

#### TPPP3 is expressed in mouse RGCs in vitro and in vivo

We analyzed TPPP3 expression patterns in RGC and RGC-depleted cultures from the retinas of P2 mice. RGC markers BRN3A and RBPMS [30, 44] as well as THY1 [3] were enriched in the pure RGC culture, along with TPPP3 (Fig. 2A). We then conducted immunostaining for *Tppp3* in the retinal cryosections of adult mice. *Tppp3* expression was localized within the RGC layer and the retinal nerve fiber layer (RNFL) (Fig. 2B and Supplementary Fig. 2). We observed that ~75% of cells co-express the RGC marker *Brn3a* and *Tppp3* (Fig. 2B). The expression of *Tppp3* within the GCL and RNFL was confirmed by immunofluorescence (Fig. 2B and Supplementary

Fig. 2) and validated by western blot analysis (Figs. 2A and 3F).

To further investigate the localization of *Tppp3* within RGCs, we conducted immunostaining for *Tppp3* in P2 primary mouse RGCs. Immunostaining images revealed that *Tppp3* was primarily expressed in RGC soma, with a low expression level in neurites. Additionally, co-labeling experiments using a neuronal marker for anti- $\beta$ -III-tubulin antibody-E7 confirmed the co-localization of *Tppp3* with  $\beta$ -III-tubulin in primary RGCs (Fig. 2C).

To understand the expression pattern of *Tppp3* in the developing retinas, we used RNAscope to probe *Tppp3* RNA expression from E12 to P0. *Tppp3* expression was detected in the inner retinal layer at E12 and specifically within the ganglion cell layer at P0 (Fig. 2D). Total RNA data indicated that *Tppp3* expression exhibited the highest levels at E14.5, coinciding with the peak of RGC differentiation (Fig. 2D), similar to the expression pattern of *Brn3a* [41]. These findings strongly support the hypothesis that *Tppp3* is a novel RGC marker.

#### TPPP3 enhances RGC neurite outgrowth ex vivo

Since previous studies have implicated *Tppp3* in zebrafish axon regeneration [20], we first investigated if *Tppp3* promotes neurite outgrowth ex vivo. We transduced primary mouse RGCs by adding AAV2-*Tppp3*-OE or control AAV2, or with an AAV2 vector containing *Tppp3* shRNA (AAV2-sh*Tppp3*) or AAV2 of scramble shRNA to the culture medium. Quantitative analysis of the longest neurite from each RGC revealed that *Tppp3* overexpression led to a significant enhancement in neurite outgrowth by approximately 20% compared to control conditions (Fig. 2E). Conversely, *Tppp3* knockdown resulted in a significant reduction in neurite outgrowth by around 20% relative to controls (Fig. 2F). To validate the effectiveness of the AAV2-sh*Tppp3*, we treated HeLa cells with *Tppp3*-OE AAV2, followed by transduction with control shRNA AAV2 or *Tppp3* shRNA AAV2. Protein analysis confirmed a significant knockdown of TPPP3 using *Tppp3* shRNA AAV2 (Supplementary

(See figure on next page.)

**Fig. 2** TPPP3 is expressed in mouse RGCs and promotes RGC neurite outgrowth ex vivo. **A** Western blots show that RGC markers BRN3A, RBPMS, and THY1 are expressed selectively in the immunopurified RGC cell population, as is *Tppp3*. **B** Immunostaining of RGCs for BRN3A and TPPP3 in adult mouse retinal sections reveals that *Tppp3* is expressed within the RGC layer. ~75% of BRN3A+ cells co-express *Tppp3* (white arrows). Scale bar = 100  $\mu$ m. **C** Immunostaining of P2 primary RGCs shows expression of anti- $\beta$ -III-tubulin antibody E7. Co-labeling with anti- $\beta$ -III-tubulin antibody E7 and *Tppp3* confirmed that *Tppp3* is expressed primarily within the soma of RGCs. Scale bar = 50  $\mu$ m. **D** RNAscope analysis of *Tppp3* in the developing mouse eye. *Tppp3* expression reached its peak at E14.5 and subsequently decreased. **E** Representative images of primary RGCs transduced with AAV2-control or AAV2-*Tppp3*-OE vectors. Quantification of mean neurite length per cell after transduction showed that *Tppp3* overexpression increases RGC neurite outgrowth by ~20% (n = 5 independent cultures). **F** Representative images of primary RGCs transduced with AAV2-shCtrl or AAV2-sh*Tppp3* vectors. Quantification of mean neurite length per cell after transduction showed that *Tppp3* knockdown decreases neurite outgrowth by ~20%. Each data point reflects an independent cell culture. Statistical significance was determined using one sample t-test (\*\*\*\*p < 0.0001, \*\*\*p < 0.001). Mean  $\pm$  SEM is shown

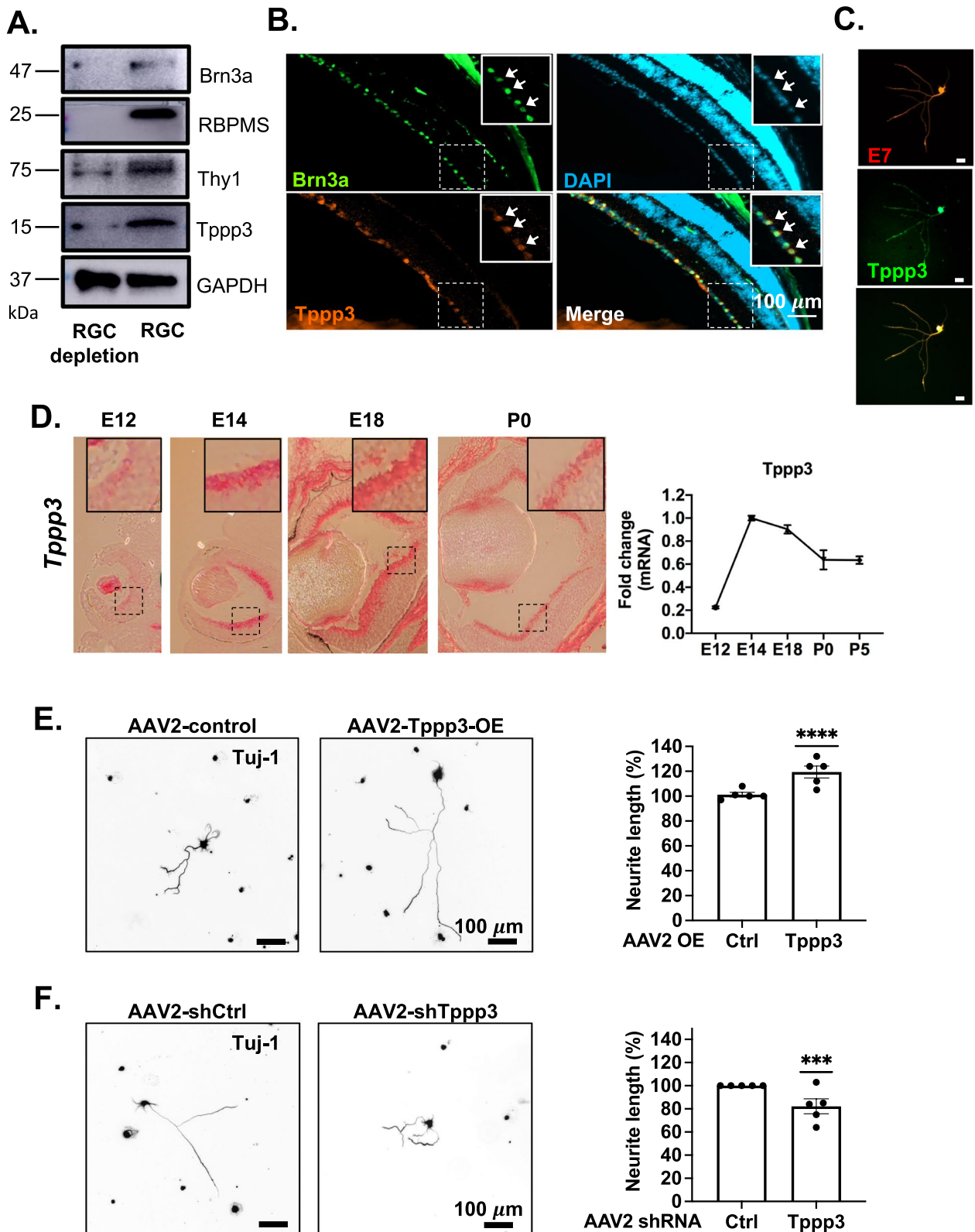


**Fig. 2** (See legend on previous page.)

Fig. 3). Collectively, these findings suggest that *Tppp3* functions as a positive regulator of neurite outgrowth in RGCs.

### **Tppp3 promotes axon regeneration and RGC survival after ONC**

Since *Tppp3* overexpression increased neurite outgrowth *ex vivo*, we next investigated the effects of *Tppp3* on axon regeneration and RGC survival *in vivo*. We intravitreally injected AAV2-*Tppp3*-OE or AAV2 control vector and allowed two weeks for protein expression (Supplementary Fig. 4). Following this, we performed ONC, and evaluated axonal regeneration and RGC survival outcomes two weeks after ONC (Fig. 3A). Additionally, we confirmed that *Tppp3* expression is affected by ONC, as its levels in purified RGCs decreased to 80% after one week and 54% after two weeks in surviving RGCs compared to non-crush controls (Fig. 1F). Our data showed that *Tppp3* overexpression significantly promotes axon regeneration, as indicated by increased CTB-555+ regenerative axon beyond the injury site compared to controls (Fig. 3B, C). In addition, the Western blot revealed that *Tppp3* protein was significantly decreased in the optic nerve after crush (Fig. 3F). These results suggest that *Tppp3* overexpression is involved in promoting axon regeneration in the retina. Next, we investigated the effect of *Tppp3* overexpression on RGC survival. We observed that >80% of RGCs are lost two weeks after ONC and *Tppp3* overexpression significantly improved RGC survival, indicating the protective role of *Tppp3* in RGCs (Figs. 3D and E). Taken together, our results demonstrate the therapeutic effects of *Tppp3* on axon regeneration and RGC survival in a mouse model of ONC.

### **Tppp3 overexpression upregulates *Bmp4* signaling and inflammation-related genes**

To gain insights into the molecular mechanisms underlying the pro-regenerative effects of *Tppp3*, we performed

bulk RNA sequencing. We analyzed gene expression profiles in AAV2-*Tppp3*-OE-transduced and control retinas two days after ONC. We chose this time point because RGC death typically initiates three–five days after ONC [53], allowing us to observe transcriptional changes before RGC death. RNA sequencing and subsequent bioinformatic analysis identified 176 differentially expressed genes, consisting of 108 upregulated genes and 68 downregulated genes in response to *Tppp3* overexpression (Fig. 4A). Expression of *Tppp3* itself exhibited a two-fold change in the whole retina two days after ONC, indicating elevated levels of *Tppp3* after intravitreal injection (data not shown).

Differential gene expression analysis revealed significant changes following *Tppp3* overexpression, including upregulation of genes related to axon regeneration, survival, eye development, and inflammation. (Fig. 4C). Notably, *Bmp4*, an enhancer of RGC survival and axon regeneration [50], was upregulated, and this result was confirmed by qPCR (Fig. 4B). These findings suggest that *Tppp3* overexpression may influence the expression of genes involved in axon regeneration and survival pathways. Additionally, we performed gene ontology (GO) analysis to explore the functional implications of differentially expressed genes. Interestingly, GO terms associated with inflammation and the BMP signaling pathway further supported the involvement of BMP signaling in the observed molecular changes (Fig. 4D). BMP2 and BMP4 have been associated with improving neurite outgrowth *in vitro* [22]. Further analysis is needed to elucidate the genetic interaction of BMP4/SMAD pathway and *Tppp3*. Additionally, *Aldh1a3*, a gene associated with retinoic acid signaling and vital for eye and neuronal development, showed increased expression two days after ONC. The upregulation of genes in the crystallin family, including *Cryaa*, *Crybb2*, *Crygc*, and *Crygs*, indicated alterations in eye development and structure. Notably, the  $\beta/\gamma$  superfamily of

(See figure on next page.)

**Fig. 3** *Tppp3* promotes axon regeneration and improves RGC survival. **A** Scheme of experimental setup for ONC and sample collection.

AAV2 vectors were intravitreally injected into eyes two weeks before ONC. Two days before sample collection, CTB-555, an anterograde tracer, was intravitreally injected into eyes to label regenerating axons. Optic nerves and retinas were collected two weeks after ONC. **B** Representative images of optic nerve sections transduced with AAV2 vectors and labeled with CTB-555. *Tppp3* overexpression significantly increases CTB-555+ axons two weeks after ONC. The crush site is marked with an asterisk. The optic nerve's proximal end (towards the eye globe) is located on the left, and the distal end (towards the brain) is on the right. Scale bar = 100  $\mu$ m. **C** Quantification of the number of CTB-555+ axons at varying distances from the crush site after transduction with AAV2-control (n = 6 optic nerves) or AAV2-*Tppp3*-OE (n = 8 optic nerves). *Tppp3* overexpression improves RGC regeneration at short distances from the crush site. Statistical significance was determined using an unpaired student's t-test for each distance (\*\**p* < 0.01). Mean  $\pm$  SEM is shown. **D** Representative images of RBPMS+ cells in flatmount retinas of **(D i)** negative controls without AAV transduction and ONC, or transduced with **(D ii)** AAV-CMV or **(D iii)** AAV-*Tppp3*-OE. Scale bar = 50  $\mu$ m. **E** *Tppp3* overexpression improves RGC survival following ONC. Quantification of the mean number of RBPMS+RGCs in flatmount retinas after transduction with control AAV2-CMV or AAV2-*Tppp3*-OE, compared to the negative control without AAV2 transduction and ONC (n = 6 retinas). Statistical significance was determined using an unpaired student's t-test (\*\*\*\**p* < 0.0001, \*\**p* < 0.01). Mean  $\pm$  SEM is shown. **F** *Tppp3* protein expression is significantly decreased in the optic nerve after ONC compared to sham control

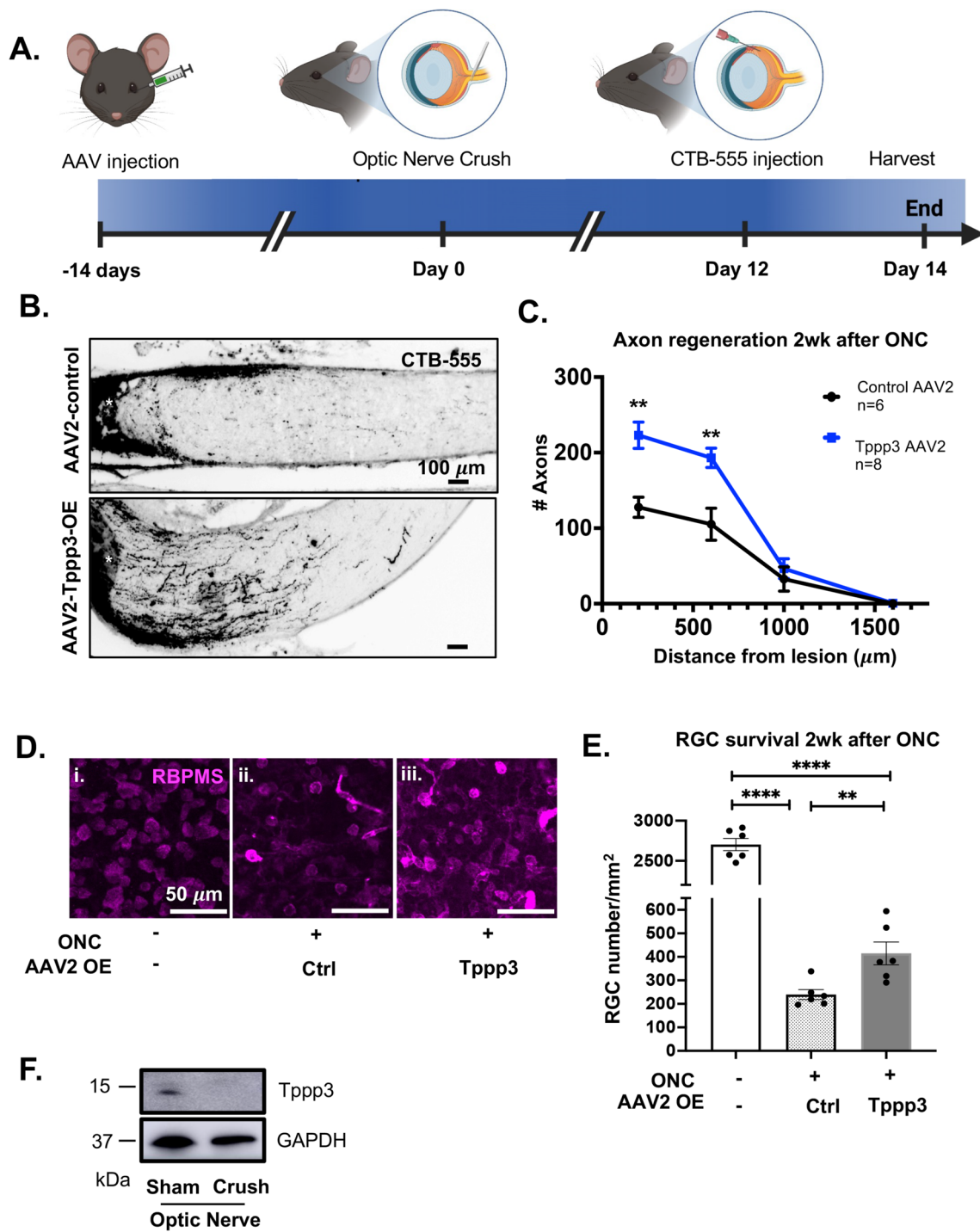


**Fig. 3** (See legend on previous page.)

crystallin, particularly *Crybb2*, was upregulated, consistent with the known protective role of crystallins neuroprotective role in the retina and their supportive function in axon regeneration [25, 39, 49]. In addition,

various chemokine and inflammation-related genes (e.g., *Ccl3*, *Ccl7*, *Cd163*, *Cd69*, *Cxcl10*, *Ifit1*, *Sele*) were upregulated two days after ONC. The upregulation of inflammation-related genes suggests that these changes

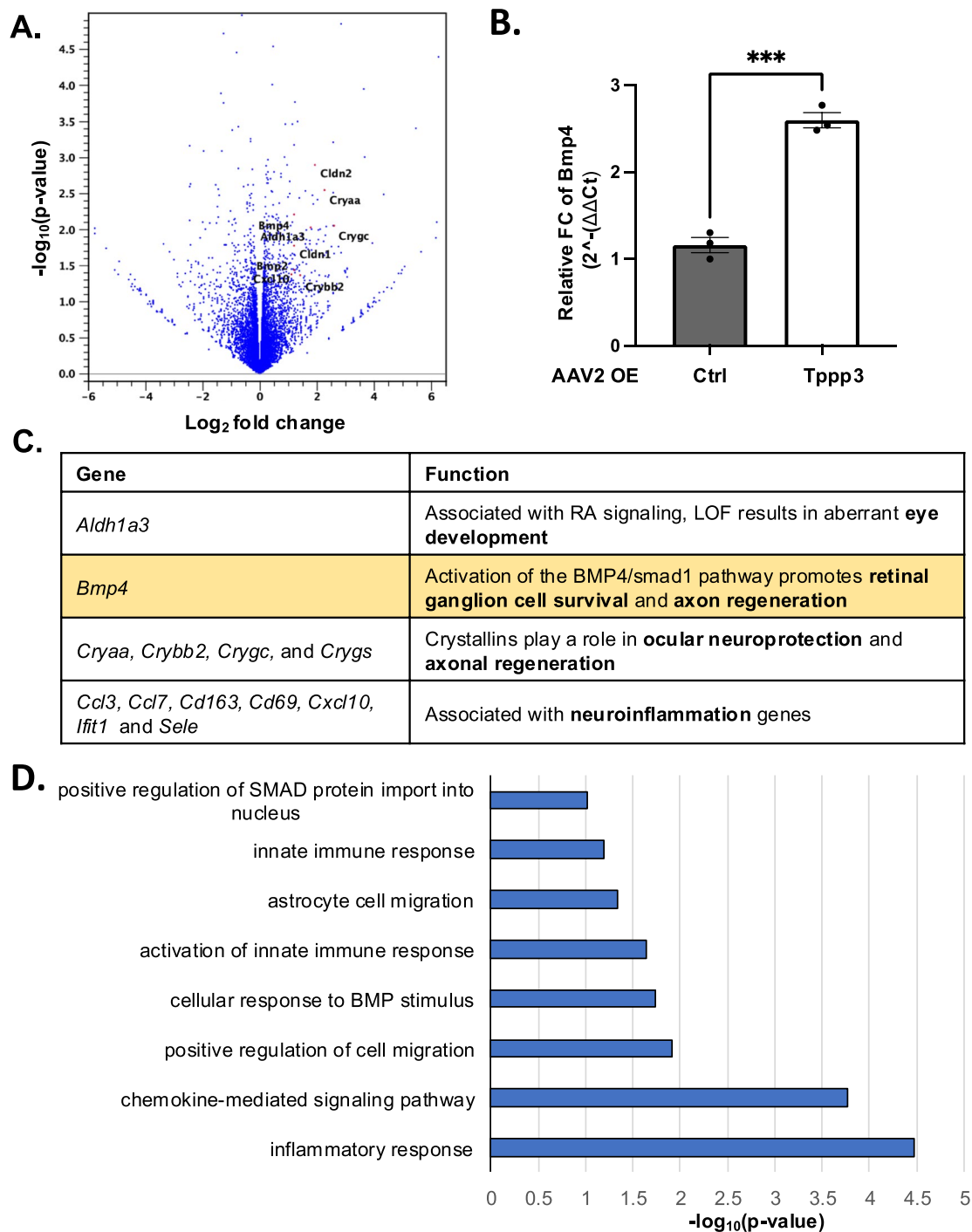


**Fig. 4** Tpp3 overexpression increases *Bmp4* and inflammation-related genes expression. **A, C** Several genes related to axon regeneration and survival were upregulated after transduction of AAV2-Tpp3-OE in the whole retina two days after ONC. **B** Real-time qPCR data comparing changes in mRNA gene expression (relative to *Gapdh* housekeeping gene) showed significantly increased *Bmp4* expression two days after ONC (n = 3 retinas). Statistical significance was determined using an unpaired student’s t-test (\*\**p* < 0.001). Mean ± SEM is shown. **D** Identified GO terms that highlight terms related to inflammation and BMP signaling increase after Tpp3 overexpression

may contribute to the regenerative effects of *Tppp3* rather than being a direct consequence of ONC injury.

Overall, our results demonstrate that *Tppp3* overexpression in the retina following ONC leads to significantly altered gene expression. Upregulation of genes related to axon regeneration and survival, such as *Bmp4*, suggests their potential role in mediating the regenerative effects of *Tppp3*. These findings contribute to our understanding of the molecular mechanisms underlying *Tppp3*-induced neural regeneration.

### Discussion

This study provides significant insights into the identification of *Tppp3* as a novel RGC marker and its functional role in axon regeneration (Fig. 5). Using scRNA sequencing on mouse retinal progenitor cells treated with PBS or GDF11, we discovered that *Tppp3* is highly expressed within the RGC-specific cluster. Its reduction with GDF11 treatment highlights its potential role in RGC fate regulation. *Tppp3* expression was localized primarily within the RGC layer, with high expression levels in the cytoplasm of RGC somas. Reanalysis of scRNA-seq data revealed that *Tppp3* expression is widespread across all RGC sub-clusters in mice [53] and expressed within the RGC clusters of macaque and human [35, 59]. Our in vitro experiments indicated that *Tppp3* acts as a positive regulator of neurite outgrowth. Furthermore, *Tppp3* overexpression in mice resulted in enhanced axonal regeneration and improved RGC survival following ONC. The role of *Tppp3* in long-distance regeneration and its potential synergistic effects with complementary

treatments must be assessed to advance the therapeutic applications of *Tppp3*.

BMP signaling has been associated with axon regeneration and RGC survival [14, 50]. GO term analysis suggests that there is a cellular response to BMP stimulus after *Tppp3* treatment. Notably, *Bmp2* and *Bmp4* were upregulated two days after ONC. Upregulation of BMPs after *Tppp3* treatment can initiate BMP signaling through SMAD-dependent canonical pathways and SMAD-independent pathways [56, 65]. BMP receptors initiate signaling by phosphorylating SMAD1, which then forms a complex with SMAD4. This SMAD1/4 complex translocates to the nucleus, where it acts as a transcriptional regulator to regulate gene expression. This signaling pathway activates GAP-43, a protein crucial for axonal growth and regeneration, thereby enhancing neuronal repair [37]. BMP4/SMAD1 pathway has been shown to enhance axon regeneration and RGC survival [50]. Although SMAD1 phosphorylation has been shown to play a key role in neurite outgrowth, its role has not been assessed yet; we cannot confidently confirm whether BMP4 signaling is activated via canonical or non-canonical pathways. The pathological and physiological functions of *Tppp3* within the retina and its relationship with BMPs are unknown. Further experiments utilizing a BMP4 inhibitor (Noggin or BMP inhibitor-LDN-193189) will help confirm the association between *Tppp3* and BMP4 signaling in RGC survival and regeneration.

While inflammation is expected after ONC, previous studies show that neuroinflammation creates an environment that supports axonal regeneration and improves

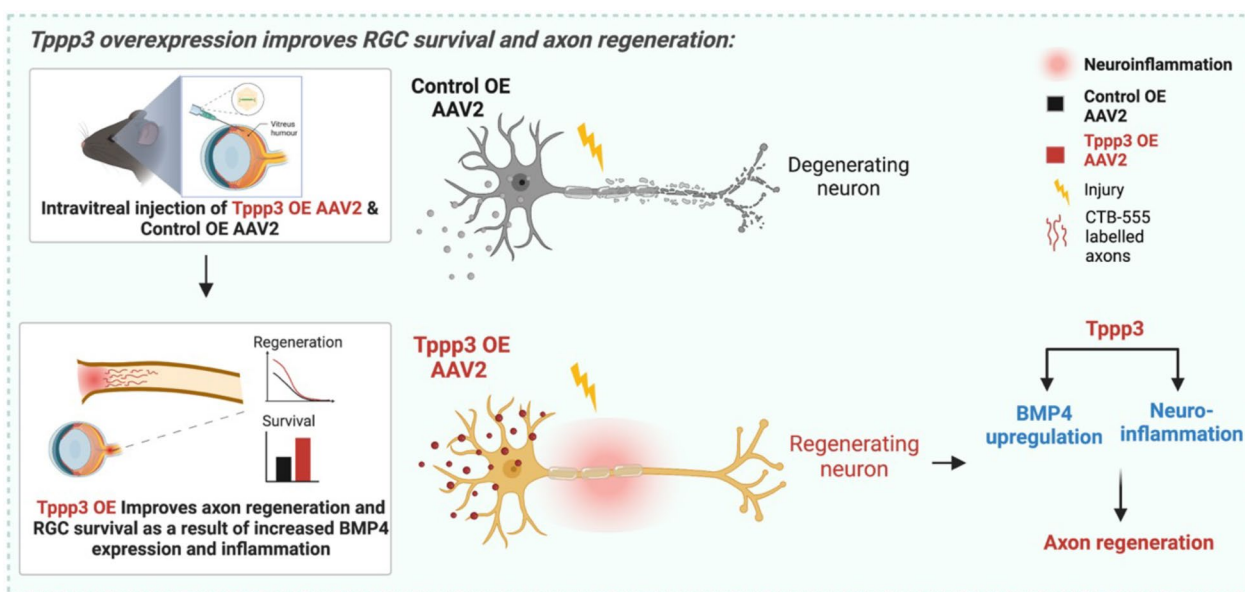


**Fig. 5** Model of *Tppp3*'s role in CNS axonal regeneration. Graphic created with BioRender.com

RGC survival [2, 7, 23, 58, 63]. For example, CXCL12, also known as SDF-1, is an inflammatory mediator that significantly promotes axon regeneration [60]. Interestingly, another study demonstrated that inhibiting microglia activation effectively prevents the loss of RGCs, possibly by suppressing pro-inflammatory cytokines within the microenvironment [42]. Since we observed enhanced axon regeneration after *Tppp3* overexpression, inflammatory genes might provide a protective environment and mediate the regenerative effects of *Tppp3*.

Injury to CNS neurons results in the formation of a retraction bulb at the tip of the injured axon [13, 52]. Retraction bulbs have disassembled and disoriented microtubules [13]. Unlike peripheral nervous system axons that develop growth cones and exhibit regeneration, CNS axons fail to regenerate after retraction bulb formation [13]. Modulation of microtubule polymerization has been shown to help develop a growth cone and promote regeneration of CNS axons [18, 46]. TPPP3 binds to tubulin and stabilizes and polymerizes microtubules [33]. It acts as a microtubule-associated protein, affecting microtubule structure and dynamics by increasing acetylation levels [51]. Tubulin polymerization has been shown to increase following neurofilament loss after axotomy [26]. Since axon regeneration relies on cytoskeleton remodeling [6], modulating cytoskeleton dynamics in injured axons facilitates the transformation of the retraction bulb into a growth-competent growth cone. Therefore, an alternative mechanism underlying axon regeneration following *Tppp3* overexpression might involve its impact on microtubulin dynamics. Since *Tppp3* treatment promotes RGC axon regeneration, it may play a role in microtubule aggregation by tubulin polymerization and/or acetylation upon ONC. Further investigation is necessary to understand the effects of *Tppp3* overexpression on microtubules after ONC.

To achieve clinically promising gene therapies to treat neural injuries, it is vital to achieve long-distance axon regeneration with functional connectivity. Although *Tppp3* overexpression indeed improves axon regeneration, it's only short-distance regeneration. *Tppp3* treatment should be continued for longer periods after injury to further evaluate the long term neuroregenerative effects. To achieve long-distance axon regeneration, a combination of genetic and molecular interventions is necessary. In a recent study, RNA sequencing analysis was performed on purified RGCs following ONC using a pro-regenerative combination treatment involving PTEN knock-down, neutrophil-derived growth factor oncomodulin (Ocm), and the non-hydrolyzable,

membrane-permeable cAMP analog CPT-cAMP (a co-factor of Ocm) [12]. Interestingly, we found that the log fold change of *Tppp3* increased after this combinatorial treatment, suggesting that *Tppp3* might be a downstream molecule of Pten signaling for promoting axon regeneration. Notably, one of the most robust effects on axon regeneration was observed through the co-deletion of PTEN and SOCS3 compared to a single deletion [48]. Thus, a combination therapy using PTEN deletion and *Tppp3* overexpression would hold the promise of improving long-distance axon regeneration. Conversely, investigating the effects of *Tppp3* on axonal degeneration would provide valuable insights into whether, in addition to promoting regeneration, it also plays a protective role by delaying axonal degeneration. Future experiments, utilizing *Tppp3* and other pro-regenerative combination treatments are imperative to unravel the precise role of *Tppp3* in the regulatory cascade governing axon regeneration.

TPPPP3 expression is also elevated in various cancer types, and knockdown of *Tppp3* transcripts suppresses tumor cell proliferation and migration [24, 43, 47, 62, 66, 67]. Interestingly, many tumor-relevant genes such as *PTEN* [28] and *KLF9* [27] are associated with axon regeneration [29, 38]. As elevated *Tppp3* levels can promote cell proliferation and migration, the long-term effects of *Tppp3* overexpression remain unknown. Future studies need to investigate whether overexpressing *Tppp3* induces an oncogenic-like state. Furthermore, it's important to conduct a thorough assessment of *Tppp3*'s potential oncogenic role before advancing to preclinical trials.

## Conclusions

Our study utilizes acute optic neuropathy to investigate the effects of *Tppp3* overexpression on RGC survival and axon regeneration. *Tppp3* could potentially serve as a therapeutic agent to enhance optic nerve regeneration and preserve RGC function in CNS injuries. To enhance our understanding of *Tppp3* in glaucoma, incorporating chronic injury models [36] such as intraocular pressure elevation and reperfusion would be an important future work. Further investigations into the underlying mechanisms of *Tppp3* may reveal additional therapeutic targets and pathways for interventions in other CNS injuries and neurodegenerative diseases.

## Abbreviations

CNS	Central nervous system
CTB-555	Cholera toxin subunit B (CTB)-conjugated Alexa Fluor 555 (CTB-555)
GDF	Growth and differentiation factors
ONC	Optic nerve crush

RGCs	Retinal ganglion cells
scRNA-seq	Single-cell RNA sequencing
Tppp3	Tubulin polymerization promoting protein family member 3

## Supplementary Information

The online version contains supplementary material available at <https://doi.org/10.1186/s40478-024-01917-6>.

Supplementary material 1.

Supplementary material 2.

### Acknowledgements

The authors are grateful to Drs. Larry Benowitz, Susana da Silva, Takaaki Kuwajima, and Issam AlDiri for their comments and scientific discussion. We thank the University of Pittsburgh Ophthalmology Core Facilities, including Dr. Paul Kinchington (Molecular Biology Core), Kira Lathrop (Imaging Core), Katherine Davoli (Histology Core), and the Health Sciences Library System for their advice on RNA sequencing analysis. CLC Genomics Workbench and Ingenuity Pathway Analysis are licensed through the Molecular Biology Information Service of the Health Sciences Library System at the University of Pittsburgh.

### Author contributions

Conceptualization, MR and KCC; methodology, MR and KCC; investigation, MR, ZL, CYC, CHL, SW, and KCC; formal analysis, MR, ZL, CYC, MN, BT, AV, and KCC; resources, LB, JLG, JAS; writing—original draft, MR; writing—review & editing, MR and KCC; supervision, JAS, KCC; funding acquisition, LB, JLG, and KCC.

### Funding

The work was supported by the National Institutes of Health [Core Grants P30-EY008098 and P30-EY026877; R01-EY032416 (JLG), UG3MH120094 (LB)]; Eye and Ear Foundation of Pittsburgh; an unrestricted grant and a career development award from Research to Prevent Blindness (KCC); an Individual Investigator Award from Foundation Fighting Blindness (LB); the UPMC Immune Transplant and Therapy Center (LB); a Shaffer Grant from Glaucoma Research Foundation (KCC).

### Availability of data and materials

RNA sequencing data generated from this study have been deposited in the GEO database with the accession number- GSE24244756. scRNA sequencing data generated in this study can be accessed via the accession number- GSE252861. The remaining scRNA sequencing data came from previously published studies, as highlighted in the manuscript, and the accession numbers are listed in the methods sections. The datasets will be made publicly available as of the date of publication. This paper does not report the original code. Any additional information required to reanalyze the data reported in this paper is available from the lead contact upon request. Further information and requests for resources and reagents should be directed to and will be fulfilled by the lead contact, Kun-Che Chang (kcchang@pitt.edu).

### Declarations

#### Ethics approval and consent to participate

The study was conducted in compliance with the ARVO guidelines and approved by IACUC at the University of Pittsburgh.

#### Consent for publication

Not applicable.

#### Competing interests

KCC and JLG are co-inventors on a patent application submitted through Stanford University. The authors declare no other competing interests.

Received: 8 August 2024 Accepted: 14 December 2024

Published online: 29 December 2024

### References

- Aoki M, Segawa H, Naito M, Okamoto H (2014) Identification of possible downstream genes required for the extension of peripheral axons in primary sensory neurons. *Biochem Biophys Res Commun* 445:357–362. <https://doi.org/10.1016/j.bbrc.2014.01.193>
- Au NP, Ma CHE (2022) Neuroinflammation, microglia and implications for retinal ganglion cell survival and axon regeneration in traumatic optic neuropathy. *Front Immunol* 13:860070. <https://doi.org/10.3389/fimmu.2022.860070>
- Barnstable CJ, Drager UC (1984) Thy-1 antigen: a ganglion cell specific marker in rodent retina. *Neuroscience* 11:847–855. [https://doi.org/10.1016/0306-4522\(84\)90195-7](https://doi.org/10.1016/0306-4522(84)90195-7)
- Barres BA, Silverstein BE, Corey DP, Chun LL (1988) Immunological, morphological, and electrophysiological variation among retinal ganglion cells purified by panning. *Neuron* 1:791–803. [https://doi.org/10.1016/0896-6273\(88\)90127-4](https://doi.org/10.1016/0896-6273(88)90127-4)
- Benowitz LI, He Z, Goldberg JL (2017) Reaching the brain: advances in optic nerve regeneration. *Exp Neurol* 287:365–373. <https://doi.org/10.1016/j.expneurol.2015.12.015>
- Blanquie O, Bradke F (2018) Cytoskeleton dynamics in axon regeneration. *Curr Opin Neurobiol* 51:60–69. <https://doi.org/10.1016/j.conb.2018.02.024>
- Bollaerts I, Van Houcke J, Andries L, De Groef L, Moons L (2017) Neuroinflammation as fuel for axonal regeneration in the injured vertebrate central nervous system. *Mediators Inflamm* 2017:9478542. <https://doi.org/10.1155/2017/9478542>
- Bradke F, Fawcett JW, Spira ME (2012) Assembly of a new growth cone after axotomy: the precursor to axon regeneration. *Nat Rev Neurosci* 13:183–193. <https://doi.org/10.1038/nrn3176>
- Cameron EG, Xia X, Galvao J, Ashouri M, Kapiloff MS, Goldberg JL (2020) Optic nerve crush in mice to study retinal ganglion cell survival and regeneration. *Bio Protoc*. <https://doi.org/10.21769/BioProtoc.3559>
- Chang KC, Bian M, Xia X, Madaan A, Sun C, Wang Q, Li L, Nahmou M, Noro T, Yokota S et al (2021) Posttranslational modification of Sox11 regulates RGC survival and axon regeneration. *ENeuro* : <https://doi.org/10.1523/ENEURO.0358-20.2020>
- Chang KC, Sun C, Cameron EG, Madaan A, Wu S, Xia X, Zhang X, Tenerelli K, Nahmou M, Knasel CM et al (2019) Opposing effects of growth and differentiation factors in cell-fate specification. *Curr Biol* 29(1963–1975):e1965. <https://doi.org/10.1016/j.cub.2019.05.011>
- Cheng Y, Yin Y, Zhang A, Bernstein AM, Kawaguchi R, Gao K, Potter K, Gilbert HY, Ao Y, Ou J et al (2022) Transcription factor network analysis identifies REST/NRSF as an intrinsic regulator of CNS regeneration in mice. *Nat Commun* 13:4418. <https://doi.org/10.1038/s41467-022-31960-7>
- Erturk A, Hellal F, Enes J, Bradke F (2007) Disorganized microtubules underlie the formation of retraction bulbs and the failure of axonal regeneration. *J Neurosci* 27:9169–9180. <https://doi.org/10.1523/JNEUROSCI.0612-07.2007>
- Farrukh F, Davies E, Berry M, Logan A, Ahmed Z (2019) BMP4/Smad1 signalling promotes spinal dorsal column axon regeneration and functional recovery after injury. *Mol Neurobiol* 56:6807–6819. <https://doi.org/10.1007/s12035-019-1555-9>
- Fawcett JW (2020) The struggle to make CNS axons regenerate: why has it been so difficult? *Neurochem Res* 45:144–158. <https://doi.org/10.1007/s11064-019-02844-y>
- Fu MM, McAlear TS, Nguyen H, Oses-Prieto JA, Valenzuela A, Shi RD, Perrino JJ, Huang TT, Burlingame AL, Bechstedt S et al (2019) The Golgi outpost protein TPPP nucleates microtubules and is critical for myelination. *Cell* 179(132–146):e114. <https://doi.org/10.1016/j.cell.2019.08.025>
- He Z, Jin Y (2016) Intrinsic control of axon regeneration. *Neuron* 90:437–451. <https://doi.org/10.1016/j.neuron.2016.04.022>

18. Hellal F, Hurtado A, Ruschel J, Flynn KC, Laskowski CJ, Umlauf M, Kapitein LC, Strikis D, Lemmon V, Bixby J et al (2011) Microtubule stabilization reduces scarring and causes axon regeneration after spinal cord injury. *Science* 331:928–931. <https://doi.org/10.1126/science.1201148>
19. Howell GR, Soto I, Libby RT, John SW (2013) Intrinsic axonal degeneration pathways are critical for glaucomatous damage. *Exp Neurol* 246:54–61. <https://doi.org/10.1016/j.expneurol.2012.01.014>
20. Huang R, Chen M, Yang L, Wagle M, Guo S, Hu B (2017) MicroRNA-133b negatively regulates zebrafish single mauthner-cell axon regeneration through targeting tppp3 in vivo. *Front Mol Neurosci* 10:375. <https://doi.org/10.3389/fnmol.2017.00375>
21. Judit O, Attila L, Tibor S, Tímea B, Judit O (2022) Modulatory role of TPPP3 in microtubule organization and its impact on alpha-synuclein pathology. *Cells*. <https://doi.org/10.3390/cells11193025>
22. Kerrison JB, Lewis RN, Otteson DC, Zack DJ (2005) Bone morphogenetic proteins promote neurite outgrowth in retinal ganglion cells. *Mol Vis* 11:208–215
23. Leon S, Yin Y, Nguyen J, Irwin N, Benowitz LI (2000) Lens injury stimulates axon regeneration in the mature rat optic nerve. *J Neurosci* 20:4615–4626. <https://doi.org/10.1523/JNEUROSCI.20-12-04615.2000>
24. Li Y, Bai M, Xu Y, Zhao W, Liu N, Yu J (2018) TPPP3 promotes cell proliferation, invasion and tumor metastasis via STAT3/twist1 pathway in non-small-cell lung carcinoma. *Cell Physiol Biochem* 50:2004–2016. <https://doi.org/10.1159/000494892>
25. Liedtke T, Schwamborn JC, Schroer U, Thanos S (2007) Elongation of axons during regeneration involves retinal crystallin beta b2 (crybb2). *Mol Cell Proteom* 6:895–907. <https://doi.org/10.1074/mcp.M600245-MCP200>
26. Lund LM, Machado VM, McQuarrie IG (2002) Increased beta-actin and tubulin polymerization in regrowing axons: relationship to the conditioning lesion effect. *Exp Neurol* 178:306–312. <https://doi.org/10.1006/exnr.2002.8034>
27. Mao Z, Fan X, Zhang J, Wang X, Ma X, Michalski CW, Zhang Y (2017) KLF9 is a prognostic indicator in human pancreatic ductal adenocarcinoma. *Anticancer Res* 37:3795–3799. <https://doi.org/10.21873/anticancer.11756>
28. Milella M, Falcone I, Conciatori F, Cesta Incani U, Del Curatolo A, Inzerilli N, Nuzzo CM, Vaccaro V, Vari S, Cognetti F et al (2015) PTEN: multiple functions in human malignant tumors. *Front Oncol* 5:24. <https://doi.org/10.3389/fonc.2015.00024>
29. Moore DL, Blackmore MG, Hu Y, Kaestner KH, Bixby JL, Lemmon VP, Goldberg JL (2009) KLF family members regulate intrinsic axon regeneration ability. *Science* 326:298–301. <https://doi.org/10.1126/science.1175737>
30. Nadal-Nicolas FM, Jimenez-Lopez M, Sobrado-Calvo P, Nieto-Lopez L, Canovas-Martinez I, Salinas-Navarro M, Vidal-Sanz M, Agudo M (2009) Brn3a as a marker of retinal ganglion cells: qualitative and quantitative time course studies in naive and optic nerve-injured retinas. *Invest Ophthalmol Vis Sci* 50:3860–3868. <https://doi.org/10.1167/iovs.08-3267>
31. Nawabi H, Belin S, Cartoni R, Williams PR, Wang C, Latremoliere A, Wang X, Zhu J, Taub DG, Fu X et al (2015) Doublecortin-like kinases promote neuronal survival and induce growth cone reformation via distinct mechanisms. *Neuron* 88:704–719. <https://doi.org/10.1016/j.neuron.2015.10.005>
32. Olah J, Szenasi T, Szabo A, Kovacs K, Low P, Stifanic M, Orosz F (2017) Tubulin binding and polymerization promoting properties of tubulin polymerization promoting proteins are evolutionarily conserved. *Biochemistry* 56:1017–1024. <https://doi.org/10.1021/acs.biochem.6b00902>
33. Olah J, Szenasi T, Szunyogh S, Szabo A, Lehotzky A, Ovadi J (2017) Further evidence for microtubule-independent dimerization of TPPP/p25. *Sci Rep* 7:40594. <https://doi.org/10.1038/srep40594>
34. Orosz F (2012) A new protein superfamily: TPPP-like proteins. *PLoS ONE* 7:e49276. <https://doi.org/10.1371/journal.pone.0049276>
35. Ozturk BE, Johnson ME, Kleyman M, Turunc S, He J, Jabalamei S, Xi Z, Visel M, Dufour VL, Iwabe S et al (2021) scAAVengr, a transcriptome-based pipeline for quantitative ranking of engineered AAVs with single-cell resolution. *Elife*. <https://doi.org/10.7554/eLife.64175>
36. Pang IH, Clark AF (2020) Inducible rodent models of glaucoma. *Prog Retin Eye Res* 75:100799. <https://doi.org/10.1016/j.preteyeres.2019.100799>
37. Parikh P, Hao Y, Hosseinkhani M, Patil SB, Huntley GW, Tessier-Lavigne M, Zou H (2011) Regeneration of axons in injured spinal cord by activation of bone morphogenetic protein/Smad1 signaling pathway in adult neurons. *Proc Natl Acad Sci U S A* 108:E99–107. <https://doi.org/10.1073/pnas.1100426108>
38. Park KK, Liu K, Hu Y, Smith PD, Wang C, Cai B, Xu B, Connolly L, Kramvis I, Sahin M et al (2008) Promoting axon regeneration in the adult CNS by modulation of the PTEN/mTOR pathway. *Science* 322:963–966. <https://doi.org/10.1126/science.1161566>
39. Piri N, Kwong JM, Gu L, Caprioli J (2016) Heat shock proteins in the retina: focus on HSP70 and alpha crystallins in ganglion cell survival. *Prog Retin Eye Res* 52:22–46. <https://doi.org/10.1016/j.preteyeres.2016.03.001>
40. Qian C, Zhou FQ (2020) Updates and challenges of axon regeneration in the mammalian central nervous system. *J Mol Cell Biol* 12:798–806. <https://doi.org/10.1093/jmcb/mjaa026>
41. Quina LA, Pak W, Lanier J, Banwait P, Gratwick K, Liu Y, Velasquez T, O'Leary DD, Goulding M, Turner EE, Brn3a-expressing retinal ganglion cells project specifically to thalamocortical and collicular visual pathways. *J Neurosci* 25:11595–11604. <https://doi.org/10.1523/JNEUROSCI.2837-05.2005>
42. Rao M, Huang YK, Liu CC, Meadows C, Cheng HC, Zhou M, Chen YC, Xia X, Goldberg JL, Williams AM et al (2023) Aldose reductase inhibition decelerates optic nerve degeneration by alleviating retinal microglia activation. *Sci Rep* 13:5592. <https://doi.org/10.1038/s41598-023-32702-5>
43. Ren Q, Hou Y, Li X, Fan X (2020) Silence of TPPP3 suppresses cell proliferation, invasion and migration via inactivating NF-kappaB/COX2 signal pathway in breast cancer cell. *Cell Biochem Funct* 38:773–781. <https://doi.org/10.1002/cbf.3546>
44. Rodriguez AR, de Sevilla Muller LP, Brecha NC (2014) The RNA binding protein RBPMS is a selective marker of ganglion cells in the mammalian retina. *J Comp Neurol* 522:1411–1443. <https://doi.org/10.1002/cne.23521>
45. Scheib J, Hoke A (2013) Advances in peripheral nerve regeneration. *Nat Rev Neurol* 9:668–676. <https://doi.org/10.1038/nrneurol.2013.227>
46. Sengottuvel V, Leibinger M, Pfreimer M, Andreadaki A, Fischer D (2011) Taxol facilitates axon regeneration in the mature CNS. *J Neurosci* 31:2688–2699. <https://doi.org/10.1523/JNEUROSCI.4885-10.2011>
47. Shen A, Tong X, Li H, Chu L, Jin X, Ma H, Ouyang Y (2021) TPPP3 inhibits the proliferation, invasion and migration of endometrial carcinoma targeted with miR-1827. *Clin Exp Pharmacol Physiol* 48:890–901. <https://doi.org/10.1111/1440-1681.13456>
48. Sun F, Park KK, Belin S, Wang D, Lu T, Chen G, Zhang K, Yeung C, Feng G, Yankner BA et al (2011) Sustained axon regeneration induced by co-deletion of PTEN and SOCS3. *Nature* 480:372–375. <https://doi.org/10.1038/nature10594>
49. Thanos S, Bohm MR, zuHorste MM, Prokosch-Willing V, Hennig M, Bauer D, Heiligenhaus A (2014) Role of crystallins in ocular neuroprotection and axonal regeneration. *Prog Retin Eye Res* 42:145–161. <https://doi.org/10.1016/j.preteyeres.2014.06.004>
50. Thompson A, Berry M, Logan A, Ahmed Z (2019) Activation of the BMP4/Smad1 pathway promotes retinal ganglion cell survival and axon regeneration. *Invest Ophthalmol Vis Sci* 60:1748–1759. <https://doi.org/10.1167/iovs.18-26449>
51. Tokesi N, Lehotzky A, Horvath I, Szabo B, Olah J, Lau P, Ovadi J (2010) TPPP/p25 promotes tubulin acetylation by inhibiting histone deacetylase 6. *J Biol Chem* 285:17896–17906. <https://doi.org/10.1074/jbc.M109.096578>
52. Tom VJ, Steinmetz MP, Miller JH, Doller CM, Silver J (2004) Studies on the development and behavior of the dystrophic growth cone, the hallmark of regeneration failure, in an in vitro model of the glial scar and after spinal cord injury. *J Neurosci* 24:6531–6539. <https://doi.org/10.1523/JNEUROSCI.0994-04.2004>
53. Tran NM, Shekhar K, Whitney IE, Jacobi A, Benhar I, Hong G, Yan W, Adiconis X, Arnold ME, Lee JM et al (2019) Single-cell profiles of retinal ganglion cells differing in resilience to injury reveal neuroprotective genes. *Neuron* 104(1039–1055):e1012. <https://doi.org/10.1016/j.neuron.2019.11.006>
54. Vargas EJM, Matamoros AJ, Qiu J, Jan CH, Wang Q, Gorczyca D, Han TW, Weissman JS, Jan YN, Banerjee S et al (2020) The microtubule regulator ringer functions downstream from the RNA repair/splicing pathway to promote axon regeneration. *Genes Dev* 34:194–208. <https://doi.org/10.1101/gad.331330.119>
55. Vincze O, Tokesi N, Olah J, Hlavanda E, Zotter A, Horvath I, Lehotzky A, Tirian L, Medzihradzsky KF, Kovacs J et al (2006) Tubulin polymerization promoting proteins (TPPPs): members of a new family with distinct

- structures and functions. *Biochemistry* 45:13818–13826. <https://doi.org/10.1021/bi061305e>
56. Wang RN, Green J, Wang Z, Deng Y, Qiao M, Peabody M, Zhang Q, Ye J, Yan Z, Denduluri S et al (2014) Bone Morphogenetic Protein (BMP) signaling in development and human diseases. *Genes Dis* 1:87–105. <https://doi.org/10.1016/j.gendis.2014.07.005>
  57. Williams PR, Benowitz LI, Goldberg JL, He Z (2020) Axon Regeneration in the mammalian optic nerve. *Annu Rev Vis Sci* 6:195–213. <https://doi.org/10.1146/annurev-vision-022720-094953>
  58. Wong KA, Benowitz LI (2022) Retinal ganglion cell survival and axon regeneration after optic nerve injury: role of inflammation and other factors. *Int J Mol Sci*. <https://doi.org/10.3390/ijms231710179>
  59. Xi Z, Ozturk BE, Johnson ME, Turunc S, Stauffer WR, Byrne LC (2022) Quantitative single-cell transcriptome-based ranking of engineered AAVs in human retinal explants. *Mol Ther Methods Clin Dev* 25:476–489. <https://doi.org/10.1016/j.omtm.2022.04.014>
  60. Xie L, Cen LP, Li Y, Gilbert HY, Strelko O, Berlinicke C, Stavarache MA, Ma M, Wang Y, Cui Q et al (2022) Monocyte-derived SDF1 supports optic nerve regeneration and alters retinal ganglion cells' response to Pten deletion. *Proc Natl Acad Sci U S A* 119:e2113751119. <https://doi.org/10.1073/pnas.2113751119>
  61. Yazdankhah M, Shang P, Ghosh S, Hose S, Liu H, Weiss J, Fitting CS, Bhutto IA, Zigler JS Jr, Qian J et al (2021) Role of glia in optic nerve. *Prog Retin Eye Res* 81:100886. <https://doi.org/10.1016/j.preteyeres.2020.100886>
  62. Ye K, Li Y, Zhao W, Wu N, Liu N, Li R, Chen L, He M, Lu B, Wang X et al (2017) Knockdown of tubulin polymerization promoting protein family member 3 inhibits cell proliferation and invasion in human colorectal cancer. *J Cancer* 8:1750–1758. <https://doi.org/10.7150/jca.18943>
  63. Yin Y, Cui Q, Li Y, Irwin N, Fischer D, Harvey AR, Benowitz LI (2003) Macrophage-derived factors stimulate optic nerve regeneration. *J Neurosci* 23:2284–2293. <https://doi.org/10.1523/JNEUROSCI.23-06-02284.2003>
  64. Young RW (1985) Cell differentiation in the retina of the mouse. *Anat Rec* 212:199–205. <https://doi.org/10.1002/ar.1092120215>
  65. Zhong J, Zou H (2014) BMP signaling in axon regeneration. *Curr Opin Neurobiol* 27:127–134. <https://doi.org/10.1016/j.conb.2014.03.009>
  66. Zhou W, Li J, Wang X, Hu R (2010) Stable knockdown of TPPP3 by RNA interference in Lewis lung carcinoma cell inhibits tumor growth and metastasis. *Mol Cell Biochem* 343:231–238. <https://doi.org/10.1007/s11010-010-0518-2>
  67. Zhou W, Wang X, Li L, Feng X, Yang Z, Zhang W, Hu R (2010) Depletion of tubulin polymerization promoting protein family member 3 suppresses HeLa cell proliferation. *Mol Cell Biochem* 333:91–98. <https://doi.org/10.1007/s11010-009-0208-0>

## Publisher's Note

Springer Nature remains neutral with regard to jurisdictional claims in published maps and institutional affiliations.